Arch. Metall. Mater. **64** (2019), 2, 607-611

DOI: 10.24425/amm.2019.127586

SUK HOON KANG*#, CHANG-KYU RHEE*, SANGHOON NOH*, TAE KYU KIM*

SPRAY DEPOSITION OF MECHANICALLY ALLOYED F/M ODS STEEL POWDER

Thermal/cold spray deposition were used for additive manufacture of oxide dispersion strengthened (ODS) steel layers. Mechanically alloyed F/M ODS steel powders (Fe(bal.)-10Cr-1Mo-0.25Ti-0.35Y2O3 in wt.%) were sprayed by a high velocity oxygen fuel (HVOF) and cold spray methods. HVOF, as a thermal method, was used for manufacturing a 1 mm-thick ODS steel layer with a ~95% density. The source to objective distance (SOD) and feeding rate were controlled to achieve sound manufacturing. $Y_2Ti_2O_7$ nano-particles were preserved in the HVOF sprayed layer; however, unexpected Cr_2O_3 phases were frequently observed at the boundary area of the powders. A cold spray was used for manufacturing the Cr_2O_3-free layer and showed great feasibility. The density and yield of the cold spray were roughly 80% and 45%, respectively. The softening of ODS powders before the cold spray was conducted using a tube furnace of up to 1200°C. Microstructural characteristics of the cold sprayed layer were investigated by electron back-scattered diffraction (EBSD), the uniformity of deformation amount inside powders was observed.

Keywords: additive manufacture, mechanically alloyed ODS powder, HVOF, Cold spray

1. Introduction

Oxide dispersion strengthened (ODS) steels have drawn wide attention as a promising candidate in-core structural materials of the future advanced fast reactor. ODS steels have excellent resistance to creep and irradiation induced swelling [1-3]. It is well known that uniform nano-oxide dispersoids act as pinning points to obstruct dislocation and grain boundary motion in ODS steel [4-6]. Moreover, the interfaces between the particle and matrix do the roll as sinks for radiation defects. Therefore, ODS steels usually show the more stress capacity than other candidates during neutron bombardment, and the resultant cavities are formed around the dispersed oxide particles rather than at grain boundaries [7]. For years, particular attention has been paid to the fabrication of thin-walled cladding tubes of ODS steels. The outer diameter, length and wall thickness of fuel cladding tube for a sodium fast reactor (SFR) are 7.4 mm 2500 mm and 0.54 mm, respectively. The tubing process of ODS is somewhat complicate and difficult because tens of processes, pilgering, drawing and intermediate heat treatments should be conducted. Sometimes, ODS materials can be easily broken during tubing while they cannot endure the severe shear deformation. The ODS materials are inevitably brittle because they were consolidated from powders. The consolidation method of ODS materials needs to be modified/simplified for the productivity and efficiency concern.

Recently, thermal/cold spray methods are used for additive manufacture of metals. The thermal or cold spray is discriminated by the operation temperature; the threshold temperature is generally 1000°C. The development of the high velocity oxygen fuel (HVOF) process, as a thermal spray, has enabled the wide usage of metal-based components of a large variety and geometry [8,9]. The cold spray, which propels feedstock material against a substrate with enough kinetic energy to produce a dense coating or freeform at relatively low temperatures, produces deposits that are oxide-free and fully dense with acceptable mechanical properties [10-12].

The mechanically alloyed steel powders are severely work-hardened, they are much harder than base powders. Therefore, they easily bounced off the target rather than attached to it. They are basically inadequate for usual thermal/cold spray condition, the powders needs to be softened without oxidation before spray. In this study, the thermal/cold spray methods were applied to the manufacturing of mechanically alloyed ODS steel powder. The advantages and disadvantages of using thermal or cold spray have been investigated, the more adequate process conditions for mechanical properties of ODS steels are studied. Our expectation is that the manufactured components can exhibit wrought-like microstructures with near theoretical density values, and relatively thick (–50 mm) components can be built-up for further rolling process.

2. Experimental

The chemical composition of ODS powders used in this study was Fe(bal.)-10Cr-1Mo-0.25Ti-0.35Y2O3 in wt.%.

* KOREA ATOMIC ENERGY RESEARCH INSTITUTE, MATERIALS RESEARCH DIVISION, DAEDEOK-DAERO 989-111, YUSEONG, DAEJEON, 34057, KOREA

Corresponding author: shkang77@kaeri.re.kr

They were mechanically alloyed by using a high-energy miller (CM 20) at 240 rpm for 48 hours. HVOF machine named diamond jet (DJ-2600) was used to spray the ODS powders, feeding rate was 35-65 g/min, carrier gas was nitrogen, source to objective distance (SOD) was 200~300 mm, and traverse speed was 500 mm/s. A cold spray machine was also used, the temperature was 800°C, pressure was 35 bar, SOD was 32 mm, feed rate was 25 g/min and traverse speed was 50 mm/s. The softening of ODS powder was performed using tube furnace, the annealing temperature was 600°C, 800°C, 1000°C, and 1200°C, respectively. Dispersed powders were gathered using magnet, consolidated by glue and epoxy for microstructure observation. Electro-polishing were performed as the final treatment on specimens. The spray processed specimens were observed by scanning electron microscopy – electron back-scattered diffraction system (SEM-EBSD) and transmission electron microscopy (TEM). The density and yield of the spray was measured, the oxide particles in layer was identified.

3. Results and discussion

The powders for spray have to show three characters, those are adequate hardness, regular powder size, circular shape. The hardness is important because it is related to the yield of the powder deposition. The regular powder size is important because powders of different sizes have different velocity during spray, there are interferences among them. The circular shape is important because the deformation of powder become easy and the yield of deposition become higher. Mechanically alloyed powders of ODS for the thermal/cold spray and is shown in Fig. 1(a). They mostly consist of flake type powders, however, the shape become circular and homogeneous after relatively long time of mechanical alloying. The size distribution of powders is shown in Fig. 1(b), powders are sieved by a grid (<50 μm) to obtain regular size distribution. The average diameter was estimated as 30 μm, the range of sizes stretch from 5 to 50 μm. Too small powders were eliminated by Ar blowing in glove box. A tube furnace for softening of powders is shown in Fig. 1(c). Ar gas blowed across the tube furnace to prevent oxidation of powders during softening. The annealing temperature and corresponding hardness variations are shown in Fig. 1(d), the hardness of powder was reduced almost half after 1200°C softening. Cross section images of HVOF sprayed 12 specimens were shown in Fig. 2. The density and the yield of the HVOF spray have been estimated by SEM from Fig. 2(a.1) to 2(c.4). The density and the yield of layers were mostly affected by two spray conditions, one is source to objective distance (SOD), the other is feed rate of powders. SOD is related to the amount of the heat to powders. When the SOD is longer, powders are exposed to the flame with the longer time. Enough heat amount is needed for softening of powders, however, to much heat results in the formation of unexpected phases at the boundary area of powders. Feed rate is related to the density and the yield of sprayed layers, generally, the density is high and the yield is low while the feed rate is low. It is because the interference among powders increases with increasing feed rate. In Fig. 2, SOD were 200 mm for ‘a’, 250 mm for ‘b’, 300 mm for ‘c’, respectively. Feed rates were

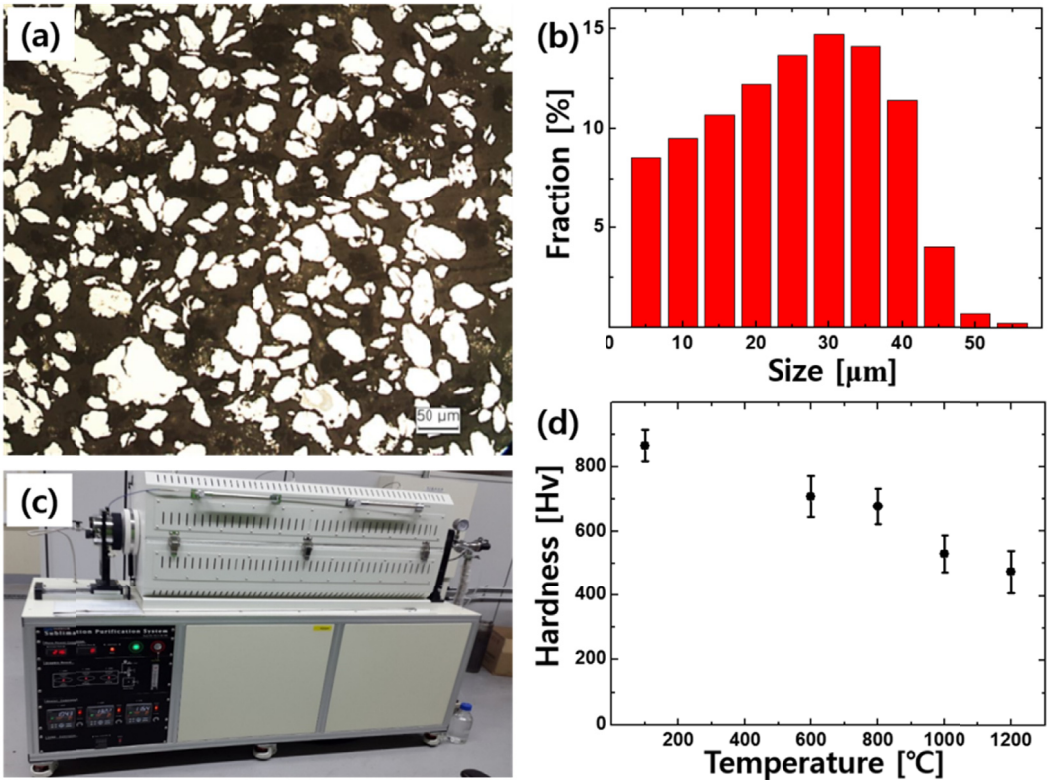

Fig. 1. (a) Mechanically alloyed powders of ODS steels for the spray processes. (b) Size distribution of mechanically alloyed powders. (c) Tube furnace for softening of powders. (d) The annealing temperature & corresponding hardness variations

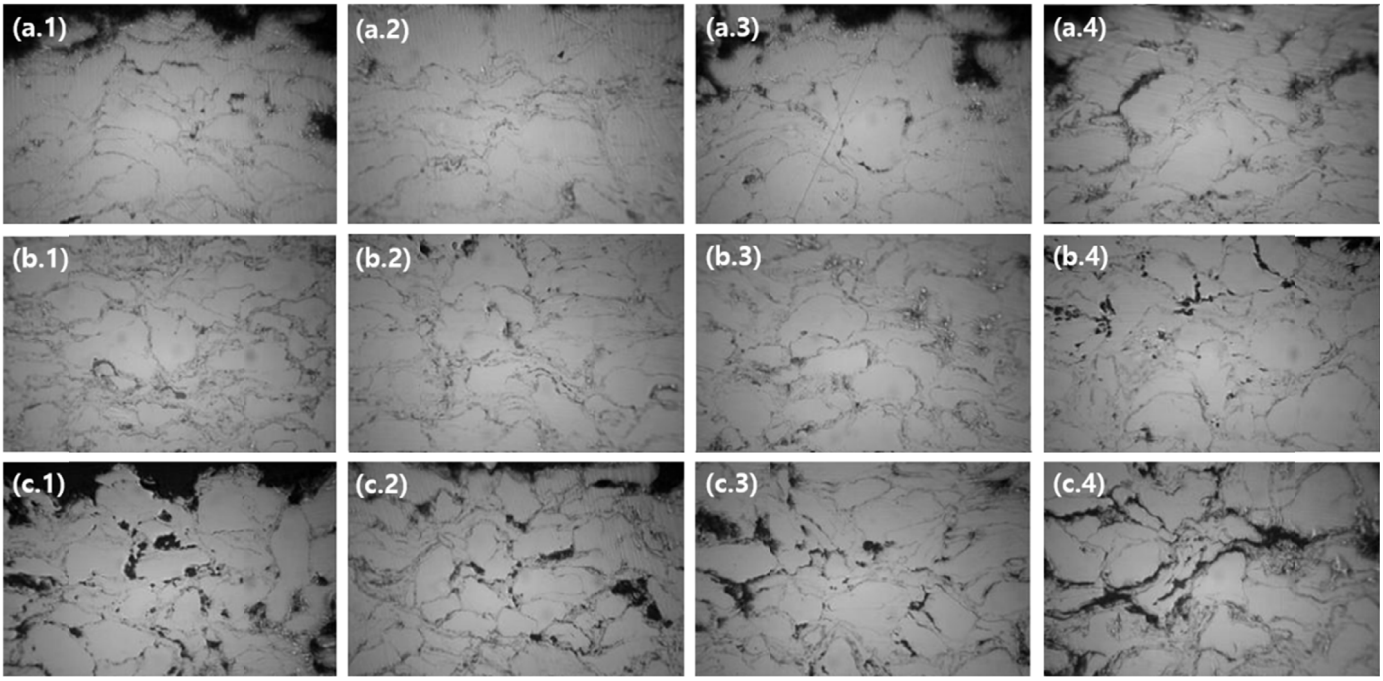

Fig. 2. SEM images of HVOF sprayed ODS layers. Source to objective distances (SOD) were 200 mm for 'a', 250 mm for 'b', 300 mm for 'c', respectively. Feed rates were 30 g/min for '1', 40 g/min for '2', 50 g/min for '3', 60 g/min for '4', respectively

30 g/min for '1', 40 g/min for '2', 50 g/min for '3', 60 g/min for '4', respectively. The density and the yield were sound while SOD is 200 ~ 250, and feed rates is 40 ~ 50, as shown in Fig. 2(a.2), 2(a.3), 2(b.2) and 2(b.3). The quantified values are plotted in Fig. 3, the density and the yield of the HVOF spray is plotted based on the observation from Fig. 2. It is shown in that open circles and rectangles (SOD values, 200 and 250 mm, respectively) are located at relatively high density and high yield position. The density was estimated 70-95%, yield was 30-55%, and it was shown that the density is inversely proportional to the yield. On the other hands, closed triangles (SOD values, 300 mm) are located at relatively low density position; it was estimated 40-65%. It was deduced that lower SOD values were effective for the higher density and yield of HVOF spray. It was also

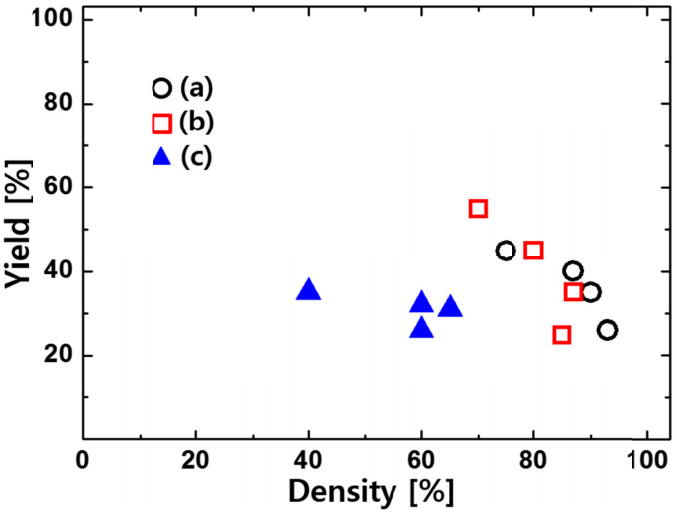

Fig. 3. The density and the yield of HVOF sprayed ODS steels. SOD is (a) 200 mm, (b) 250 mm, (c) 300 mm, respectively

estimated that the higher feed rate resulted in the lower density; however, the effect was weaker than that from the SOD values.

In Fig. 4, TEM micrographs of HVOF sprayed ODS powders are shown. Heat affected zone of ODS powders was shown with dark gray boundaries in Fig. 4(a), they represent the boundaries among powders. Each powder is plastically deformed during spray, and the gaps of powders are soundly filled with high density. However, relatively high number density of Cr_2O_3 phases was observed near by the gaps, as shown in Fig. 4(b). In Fig. 4(b), all of the oxides formed in gray compared to the relatively white Fe-ODS substrate were observed as Cr_2O_3. The evolution of Cr_2O_3 phase was disadvantageous for earning the higher density and yield of spray. Discontinuous phases can be the critical defects for the delamination of sprayed layer. Fortunately, small nano-oxide particles were preserved in the powders as shown in Fig 4(c). The high temperature of HVOF spray did not affect the nano-particles in powders, only surface area was affected. The average diameter of particles was roughly 10 nm. The phases were mostly identified as $Y_2Ti_2O_7$.

The cold sprayed ODS layer on an F/M steel plate is shown in Fig. 5. The optical micrograph from the plane view and the scanning electron micrograph from the cross section view are shown in Fig. 5(a) and 5(b), respectively. The thickness of sprayed layer was roughly ~200 μm. The density and yield of the spray were roughly 80% and 45%, respectively. The evolution of Cr_2O_3 phase was never found in any place of layers. The results were satisfactory, we expect that relatively thick components can be built-up successfully and rolling process can be conducted for obtaining the higher density of layer.

In Fig. 6, the microstructural characteristics of cold sprayed powders were displayed using a SEM-EBSD system. Fig. 6(a) ~ 6(e) are maps of band contrast, grain boundaries, subgrain

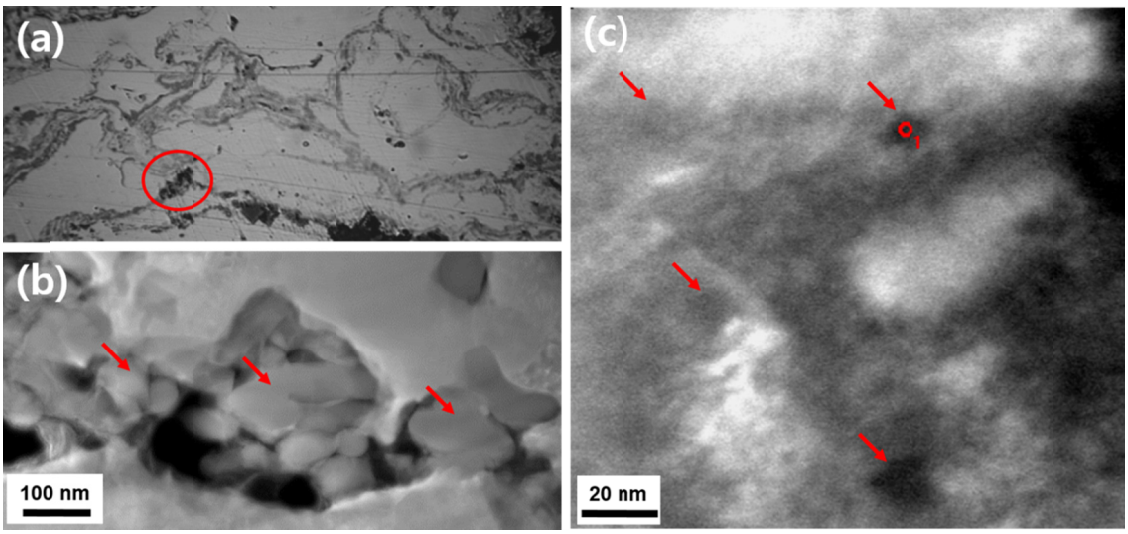

Fig. 4. Oxide particles distribution in HVOF sprayed ODS steels. (a) Heat affected zone in the coated ODS layer (b) Cr_2O_3 phases (c) $Y_2Ti_2O_7$ nano particles

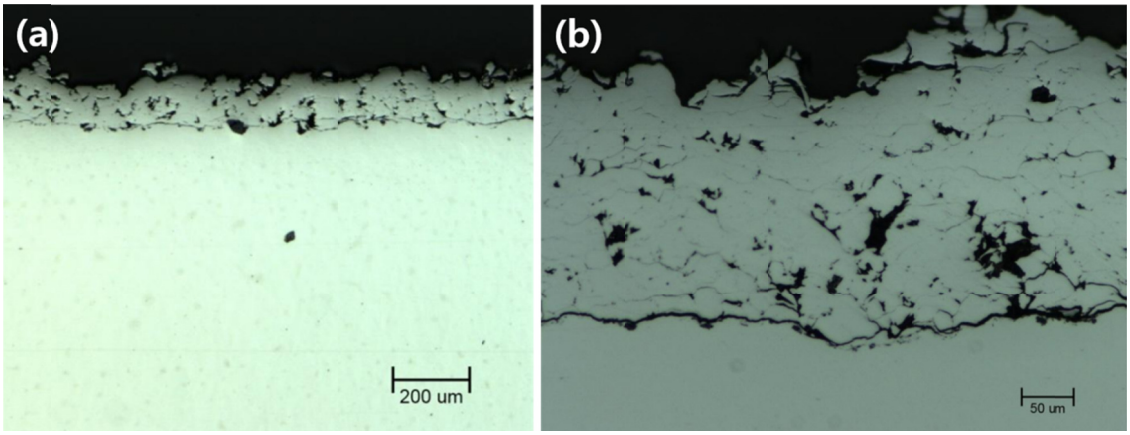

Fig. 5. Cold spray processed ODS layer. (a) Optical micrograph from the plane view. (b) Scanning electron micrograph from the cross section view

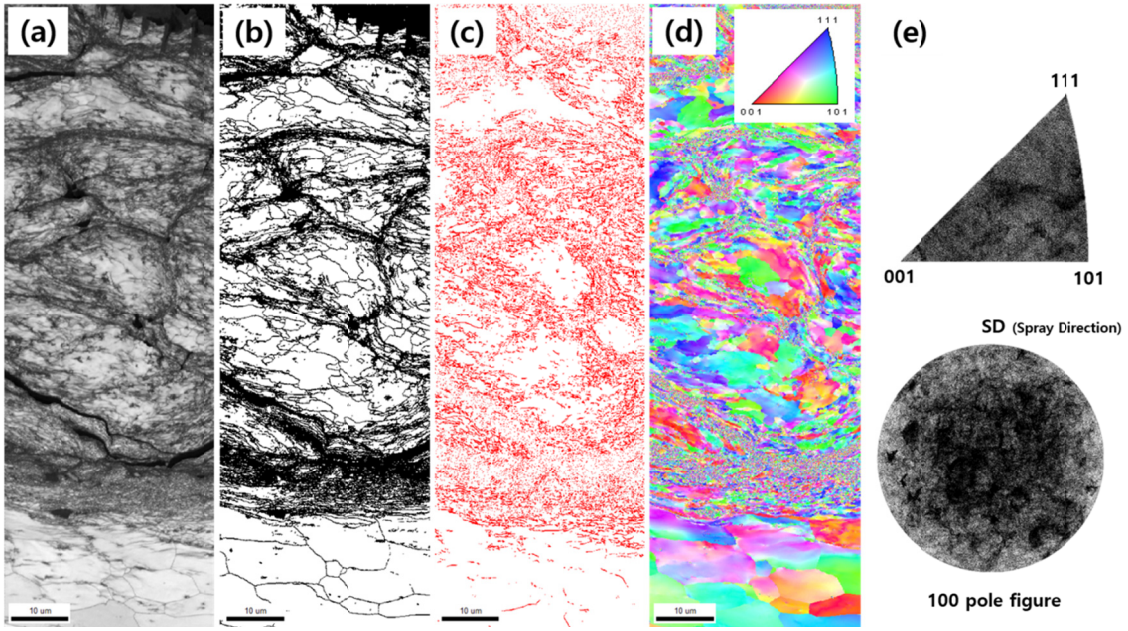

Fig. 6. Electron back-scattered diffraction (EBSD) analysis of cold spray processed ODS layer. (a) Band contrast map, (b) Grain boundary distribution map, (c) Subgrain boundary distribution map, (d) Grain orientation distribution map, (e) Inverse pole figure map along spray direction (SD) and 100 pole figure map

boundaries, orientation distribution, polefigures, respectively. The quality of EBSD pattern is usually quantified by band contrast (BC), which is derived from the average intensity of the Kikuchi bands with respect to the overall intensity within an EBSD pattern. The intensity represents the perfection of crystal structure, the intensity difference can be mapped into a gray scale image, and it describes detailed features of the microstructure as shown in Fig. 6(a). The corresponding grain and subgrain boundary distribution maps are shown in Fig. 6(b) and 6(c), respectively. The subgrain boundaries were drawn by indexing local low-angle misorientations (3-15°) in Fig. 6(c); others (>15°) were indexed as grain boundaries in Fig. 6(b). It was observed that powders are divided into small grains, subgrain boundaries are hardly observed inside each grain. The subgrain boundary distributions roughly described the dislocation density, they are only distributed along the boundaries among powders. Therefore, it is suspected that powders are recrystallized during softening process and only the boundary area is plastically deformed during cold spray. The powders need to be uniformly deformed during spray for obtaining the more density and yield. The shape and size regularity of powders and the adequate softening method need to be considered for regular deformation of powders. The orientation distribution along the spray direction (SD) is shown in Fig. 6(d), using a mixture of three primary colors – red (//<100>), green (//<110>), and blue (//<111>). The deviation angle of the orientation measurement was 5°. The indexed data showed no specific preferred orientation, colors were randomly distributed. The pole figures in the Fig. 6(e) also show no specific preferred orientation. The powders were sprayed along a specific direction, however, the grain orientations were more affected by randomly oriented recrystallization.

4. Conclusions

In this study, thermal/cold spray of mechanically alloyed F/M-ODS steel powder was investigated. HVOF was applied as one of the thermal spray method and it was very effective to produce thick film. The source to objective distance (SOD) and feeding rate were controlled to achieve the sound manufacturing. It was deduced that lower SOD values were effective for achieving the higher density and yield of HVOF spray. It was also estimated that the higher feed rate resulted in the lower density; however, the effect was weaker than that from the SOD values. $Y_2Ti_2O_7$ nano particles were found to be preserved in HVOF sprayed layer, however, unexpected Cr_2O_3 phases were frequently observed at boundary area of powders. Cold spray was used for manufacturing Cr_2O_3-free layer, it showed great feasibility. The density and yield of the cold spray were roughly 80% and 45%, respectively. The evolution of $Cr2O_3$ phase was never found in any place of layers. Microstructural characteristic of cold sprayed layer was investigated by SEM-EBSD, it was deduced that the powders need to be uniformly deformed during spray for obtaining the more density and yield. The shape and size regularity of powders and the adequate softening method need to be considered for uniform deformation of powders.

Acknowledgments

This work was supported by the Korea Institute of Energy Technology Evaluation and Planning(KETEP) and the Ministry of Trade, Industry & Energy(MOTIE) of the Republic of Korea (No. 20171510102030)

REFERENCES

[1] R. Lindau, A. Möslang, M. Rieth, M. Klimiankou, E. Materna-Morris, A. Alamo, A.-A.F. Tavassoli, C. Cayron, A.-M. Lancha, P. Fernandez, N. Baluc, R. Schäublin, E. Diegele, G. Filacchioni, J.W. Rensman, B.v.d. Schaaf, E. Lucon, W. Dietz, Fusion Eng. Des. **75-79**, 989 (2005).

[2] D.T. Hoelzer, J. Bentley, M.A. Sokolov, M.K. Miller, G.R. Odette, M.J. Alinger, J. Nucl. Mater. **367-370**, 166 (2007).

[3] A. Alamo, V. Lambard, X. Averty, M.H. Mathon, J. Nucl. Mater. **329-333**, 333 (2004).

[4] T. Yoshitake, Y. Abe, N. Akasaka, S. Ohtsuka, S. Ukai, A. Kimura, J. Nucl. Mater. **329-333,** 342 (2004).

[5] S. Noh, B.K. Choi, S.H. Kang, T.K. Kim, Nucl. Eng. Technol. **46**, 857 (2014).

[6] X. Mao, T.K. Kim, S.S. Kim, Y.S. Han, K.H. Oh, J. Jang, J. Nucl. Mater. **461**, 329 (2015).

[7] S.H. Kang, Y.-B. Chun, S. Noh, J. Jang, Y.-H. Jeong, T.K. Kim, J. Korean Phys. Soc. **66**, 505 (2015).

[8] R. Lupoi, W. O'Neill, Surface & Coatings Technology **205**, 2167 (2010).

[9] C.-J. Li, W.-Y. Li, H. Lio, J. of Thermal Spray Technology **15** (2), 212 (2006).

[10] S. Kumar, G. Bae, C. Lee, Applied Surface Science **255**, 3472 (2009).

[11] S. Yoon, H. Kim, C. Lee, Surface & Coatings Technology **201**, 9524 (2007).

[12] X.-J. Ning, J.-H. Kim, H.-J. Kim, C. Lee, Applied Surface Science **255**, 3933 (2009).